Electronic Supplementary Information

DNA nanopillar as scaffold to regulate ratio and distance of mimic enzymes for efficient cascade catalytic platform

Beibei Kou, Yaqin Chai*, Yali Yuan* and Ruo Yuan*

Key Laboratory of   Luminescence Analysis and Molecular Sensing (Southwest University),

Ministry of Education, College of Chemistry and Chemical Engineering, Southwest University,

Chongqing 400715, PR China

* Corresponding authors at: Tel.: +86 23 68252277, fax: +86 23 68253172.

E-mail addresses: yuanruo@swu.edu.cn (R. Yuan), yqchai@swu.edu.cn (Y. Q. Chai), y198688@swu.edu.cn.

EXPERIMENTAL

Materials and Reagents.

Tannic acid (TA), lead nitrate (Pb(NO$_3$)$_2$), hexanethiol (HT), dithiothreitol (DTT), N-(3-dimethylaminopropyl)-N-ethylcarbodiimide-hydrochloride (EDC) and N-hydroxy succinimide (NHS) were purchased from Sigma-Aldrich (St. Louis, MO, USA). Gold chloride (HAuCl$_4$), 3,3′,5,5′-tetramethylbenzidine (TMB), sodium citrate tribasic, hemin and K$_2$CO$_3$ were obtained from J&K Chemical Technology Co. Ltd. (Beijing, China). Alexa Fluor (AF) was acquired from Thermo Fisher Scientific (New York, USA). Ru(bpy)$_3^{2+}$ was received from Suna Tech Inc. (Suzhou, China). Carboxylated-magnetic polystyrene microspheres (PSC-COOH) was provided by Tianjin BaseLine ChromTech Research Centre (Tianjin, China). All the DNA oligonucleotides listed in Table S1 were produced by Sangon. Inc. (Shanghai, China).

**Table S1.** Sequences of the Oligonucleotides Used in This Work

Name	Sequence (from 5′ to 3′)
H$_1$	NH$_2$-(CH$_2$)$_6$ AAAGGAGAT*G* (rA) ATGTCGCCCGGGTAGGGCGGGTAGGGCGACACTGCTAGTTCGCGAGGTGCAATCTCC
L$_2$	GGTGTCTAGATCACTGTTCCTAGCAGTGT
Thiol-DNA	SH-TTTTTT
Fuel	
F$_0$	GATACTGGCAGCTCGAGAGGAGATTGCACCTCCGATAATTGCAGCTGCC
F$_1$	CATGTCGCCCATTTAACGTGATCTAGACACCCGTCACGACATGAAACCA
F$_2$	ACCCGTCATCGCAAAGTTGGAGATTGCACCTCGCATTGTCAGTGCGATG
F$_3$	TACACCTCGATTGTACCGTGATCTAGACACCACTGAAGGTGTAGCCTGA
F$_4$	CGTAAGCAGTGGTGACTCGGAGATTGCACCTCGAGATCTCCCACCACTG
Anti-fuel	
AF$_0$	GCAATTATCGGAGGTGCAATCTCCTCTCGAGCTGCCAGTATC
AF$_1$	TGGTTTCATGTCGTGACGGGTGTCTAGATCACGTTAAATGGG
AF$_2$	CTGACAATGCGAGGTGCAATCTCCAACTTTGCGATGACGGGT
PP$_5$-15A	

P$_{51}$-15A	TCGCTGAGTA**TTTT**ATGCCGAGAAATAAATTCTG**TTTT**GCAAGTGTGGGCACGCACAC**TTTT**CCTATATGGTCAACTGCTC**TTTT**CACAAATCTG**TTTT**AAAAAAAAAAAAAAA
P$_{52}$-15A	CTATCTGTAG**TTTT**ATGCCGAGAAATAAATTCTG**TTTT**TACTCAGCGACAGATTTGTG**TTTT**GTAGTAATACCAGATGGAGT**TTTT**CAACTAGCGG**TTTT**AAAAAAAAAAAAAAA
P$_{53}$-15A	CACTGGTCAG**TTTT**ATGCCGAGAAATAAATTCTG**TTTT**CTACAGATAGCCGCTAGTTG**TTTT**CGCTCTTCTATACTGGCGGA**TTTT**GGTTTGCTGA**TTTT**AAAAAAAAAAAAAAA
P$_{54}$-15A	TACCGGATCG**TTTT**ATGCCGAGAAATAAATTCTG**TTTT**CTGACCAGTGTCAGCAAACC**TTTT**CGCACCGCGACTGCGAGGAC**TTTT**CCGTAATTGC**TTTT**AAAAAAAAAAAAAAA
P$_{55}$-15A	CCACACTTGC**TTTT**ATGCCGAGAAATAAATTCTG**TTTT**CGATCCGGTAGCAATTACGG**TTTT**GCCTGGCCTTGGTCCATTTG**TTTT**GTGTGCGTGC**TTTT**AAAAAAAAAAAAAAA
R$_5$	SH-TTTTTTAGAATTTATTTCTCGGCA
PP$_5$-T$_4$	
P$_{51}$-T$_4$	ACCACTGCTTACG**TTTT**GCTGA**TTTT**GAGCAGTTGACCATATAGGA**TTTT**AGTGTACGCA**TTTT**ATGCCGAGAAATAAATTCTG**TTTT**CAATC
P$_{52}$-T$_4$	ACCACTGCTTACG**TTTT**ATCTG**TTTT**ACTCCATCTGGTATTACTACT**TTTT**TCAGCGATTG**TTTT**ACCGTGGCAGCTAACGCTTA**TTTT**ACTAG
P$_{53}$-T$_4$	ACCACTGCTTACG**TTTT**TGGTC**TTTT**TCCGCCAGTATAGAAGAGCG**TTTT**CAGATCTAGT**TTTT**CTCACAGCCAATCAGGAATG**TTTT**TTGCT
P$_{54}$-T$_4$	ACCACTGCTTACG**TTTT**CGGAT**TTTT**GTCCTCGCAGTCGCGGTGCG**TTTT**GACCAAGCAA**TTTT**GAAGCACTAAAGTTCTTTGA**TTTT**GTAAT
P$_{55}$-T$_4$	ACCACTGCTTACG**TTTT**ACACT**TTTT**CAAATGGACCAAGGCCAGGC**TTTT**ATCCGATTAC**TTTT**AGATCAAGACGTGACGAGCA**TTTT**TGCGT
QP$_4$-15A	
P$_{41}$-15A	TCGCTGAGTA**TTTT**TCCTATATGGTCAACTGCTC**TTTT**GCAAGTGTGGGCACGCACAC**TTTT**GTAGTAATACCAGATGGAGT**TTTT**CACAAATCTG**TTTT**AAAAAAAAAAAAAAA
P$_{42}$-15A	CTATCGGTAG**TTTT**TCCTATATGGTCAACTGCTC**TTTT**TACTCAGCGACAGATTTGTG**TTTT**GTAGTAATACCAGATGGAGT**TTTT**CAACTAGCGG**TTTT**AAAAAAAAAAAAAAA
P$_{43}$-15A	CACTGGTCAG**TTTT**TCCTATATGGTCAACTGCTC**TTTT**CTACCGATAGCCGCTAGTTG**TTTT**GTAGTAATACCAGATGGAGT**TTTT**GGTTTGCTGA**TTTT**AAAAAAAAAAAAAAA
P$_{44}$-15A	CCACACTTGC**TTTT**TCCTATATGGTCAACTGCTC**TTTT**CTGACCAGTGTCAGCAAACC**TTTT**GTAGTAATACCAGATGGAGT**TTTT**GTGTGCGTGC**TTTT**AAAAAAAAAAAAAAA
R$_4$	SH-TTTTTTAGCAGTTGACCATATAGG
QP$_4$-T$_4$ ($_{3, 2, 1, 0}$)	

P_{41}-T_4	ACCACTGCTTACG**TTTT**CTAAC**TTTT**ACTCCATCTGGTATTACTAC**TTTT**AC GCATGTGA**TTTT**TCCTATATGGTCAACTGCTC**TTTT**AGTCG
P_{42}-T_4	ACCACTGCTTACG**TTTT**GATCA**TTTT**ACTCCATCTGGTATTACTAC**TTTT**GT TAGCGACT**TTTT**TCCTATATGGTCAACTGCTC**TTTT**GGCTA
P_{43}-T_4	ACCACTGCTTACG**TTTT**TCGTT**TTTT**ACTCCATCTGGTATTACTAC**TTTT**TG ATCTAGCC**TTTT**TCCTATATGGTCAACTGCTC**TTTT**CTGGT
P_{44}-T_4	ACCACTGCTTACG**TTTT**TGCGT**TTTT**ACTCCATCTGGTATTACTAC**TTTT**AA CGAACCAG**TTTT**TCCTATATGGTCAACTGCTC**TTTT**TCACA
P_{41}-T_3	GCTGA**TTTT**GAGCAGTTGACCATATAGGA**TTTT**AGTGTACGCA**TTTT**GTAG TAATACCAGATGGAGT**TTTT**CAATC**TTTT**TCAGGCTACACCT
P_{42}-T_3	ATCGG**TTTT**GAGCAGTTGACCATATAGGA**TTTT**TCAGCGATTG**TTTT**GTAG TAATACCAGATGGAGT**TTTT**ACTAG**TTTT**TCAGGCTACACCT
P_{43}-T_3	TGGTC**TTTT**GAGCAGTTGACCATATAGGA**TTTT**CCGATCTAGT**TTTT**GTAG TAATACCAGATGGAGT**TTTT**TTGCT**TTTT**TCAGGCTACACCT
P_{44}-T_3	ACACT**TTTT**GAGCAGTTGACCATATAGGA**TTTT**GACCAAGCAA**TTTT**GTAG TAATACCAGATGGAGT**TTTT**TGCGT**TTTT**TCAGGCTACACCT
P_{41}-T_2	TGCGATGACGGGT**TTTT**CTAAC**TTTT**ACTCCATCTGGTATTACTAC**TTTT**AC GCATGTGA**TTTT**TCCTATATGGTCAACTGCTC**TTTT**AGTCG
P_{42}-T_2	TGCGATGACGGGT**TTTT**GATCA**TTTT**ACTCCATCTGGTATTACTAC**TTTT**GT TAGCGACT**TTTT**TCCTATATGGTCAACTGCTC**TTTT**GGCTA
P_{43}-T_2	TGCGATGACGGGT**TTTT**TCGTT**TTTT**ACTCCATCTGGTATTACTAC**TTTT**TG ATCTAGCC**TTTT**TCCTATATGGTCAACTGCTC**TTTT**CTGGT
P_{44}-T_2	TGCGATGACGGGT**TTTT**TGCGT**TTTT**ACTCCATCTGGTATTACTAC**TTTT**AA CGAACCAG**TTTT**TCCTATATGGTCAACTGCTC**TTTT**TCACA
P_{41}-T_1	GCTGA**TTTT**GAGCAGTTGACCATATAGGA**TTTT**AGTGTACGCA**TTTT**GTAG TAATACCAGATGGAGT**TTTT**CAATC**TTTT**TGGTTTCATGTCG
P_{42}-T_1	ATCGG**TTTT**GAGCAGTTGACCATATAGGA**TTTT**TCAGCGATTG**TTTT**GTAG TAATACCAGATGGAGT**TTTT**ACTAG**TTTT**TGGTTTCATGTCG
P_{43}-T_1	TGGTC**TTTT**GAGCAGTTGACCATATAGGA**TTTT**CCGATCTAGT**TTTT**GTAG TAATACCAGATGGAGT**TTTT**TTGCT**TTTT**TGGTTTCATGTCG
P_{44}-T_1	ACACT**TTTT**GAGCAGTTGACCATATAGGA**TTTT**GACCAAGCAA**TTTT**GTAG TAATACCAGATGGAGT**TTTT**TGCGT**TTTT**TGGTTTCATGTCG
P_{41}-T_0	AGCTGCCAGTATC**TTTT**CTAAC**TTTT**ACTCCATCTGGTATTACTAC**TTTT**AC GCATGTGA**TTTT**TCCTATATGGTCAACTGCTC**TTTT**AGTCG
P_{42}-T_0	AGCTGCCAGTATC**TTTT**GATCA**TTTT**ACTCCATCTGGTATTACTAC**TTTT**GT TAGCGACT**TTTT**TCCTATATGGTCAACTGCTC**TTTT**GGCTA
P_{43}-T_0	AGCTGCCAGTATC**TTTT**TCGTT**TTTT**ACTCCATCTGGTATTACTAC**TTTT**TG ATCTAGCC**TTTT**TCCTATATGGTCAACTGCTC**TTTT**CTGGT
P_{44}-T_0	AGCTGCCAGTATC**TTTT**TGCGT**TTTT**ACTCCATCTGGTATTACTAC**TTTT**AA CGAACCAG**TTTT**TCCTATATGGTCAACTGCTC**TTTT**TCACA
TP$_3$-15A	
P_{31}-15A	GCTGAGTAATAG**TTTT**TCCTATGCCGAGAAATAAATTCTG**TTTT**GCAACTG

S4

	ACCAGTGTCAGCAAACC**TTTT**GTAGTCCTATATGGTCAACTGCTC**TTTT**CACAAATCTGTC**TTTT**AAAAAAAAAAAAAAA
P$_{32}$-15A	ATCTGTAGCCGC**TTTT**TCCTATGCCGAGAAATAAATTCTGT**TTTT**CTATTACTCAGCGACAGATTTGTG**TTTT**GTAGTCCTATATGGTCAACTGCTC**TTTT**CAACTAGCGGCT**TTTT**AAAAAAAAAAAAAAA
P$_{33}$-15A	CTGGTCAGTTGC**TTTT**TCCTATGCCGAGAAATAAATTCTGT**TTTT**GCGGCTACAGATAGCCGCTAGTTG**TTTT**GTAGTCCTATATGGTCAACTGCTC**TTTT**GGTTTGCTGACA**TTTT**AAAAAAAAAAAAAAA
R$_3$	SH-TTTTTTAGAATTTATTTCTCGGCATAGG
TP$_3$-T$_4$	
P$_{31}$-T$_4$	ACCACTGCTTACG**TTTT**GCTGA**TTTT**GAGCAGTTGACCATATAGGACTAC**T****TTT**GACCAAGCAA**TTTT**TCCTATGCCGAGAAATAAATTCTGT**TTTT**CAATC
P$_{32}$-T$_4$	ACCACTGCTTACG**TTTT**ATCTG**TTTT**GAGCAGTTGACCATATAGGACTAC**T****TTT**TCAGCGATTG**TTTT**TCGCACCGTGGCAGCTAACGCTTA**TTTT**ACTAG
P$_{33}$-T$_4$	ACCACTGCTTACG**TTTT**TGGTC**TTTT**GAGCAGTTGACCATATAGGACTAC**T****TTT**CAGATCTAGT**TTTT**TCTGCTCACAGCCAATCAGGAATG**TTTT**TTGCT

Apparatus Electrochemical measurements were performed by a CHI 760E electrochemical workstation (Chenhua Instrument, Shanghai, China) with a conventional three-electrode system including a modified glassy carbon electrode (GCE, Φ = 4 mm), saturated calomel electrode and platinum wire as working, reference, counter electrode, respectively. The morphology of nanomaterials was characterized by a Tecnai G2 F30 transmission electron microscopy (TEM, USA) and atomic force microscope (AFM, Bruker, Germany). Native polyacrylamide gel electrophoresis (PAGE) was performed on a DYY-8C electrophoretic device (Beijing WoDeLife Sciences Instrument Company, Ltd.) with 8% polyacrylamide gel in 1× TBE buffer at 100 V for 1 h and gels image was carried out on Bio-Rad imaging system (Hercules, CA, U.S.A.). The UV-vis spectra was performed with a UV-2450 UV-vis spectrophotometer (Shimadzu, Tokyo, Japan). The spooling ECL spectra of Ru(bpy)$_3^{2+}$/AF system was measured on a ECL spectrometer (provided by Shandong University).
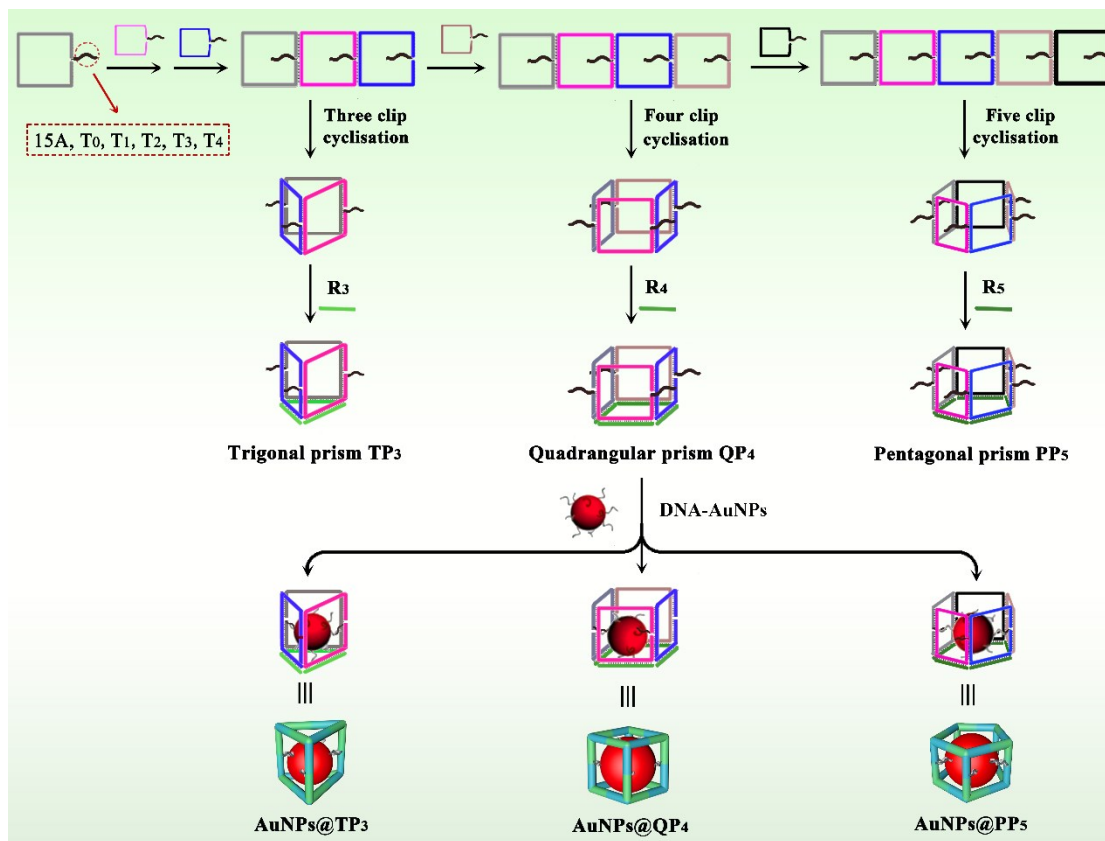
Scheme S1.Clip-by-clip approach for self-assembly of various DNA cages and the encapsulation

of DNA-AuNPs.
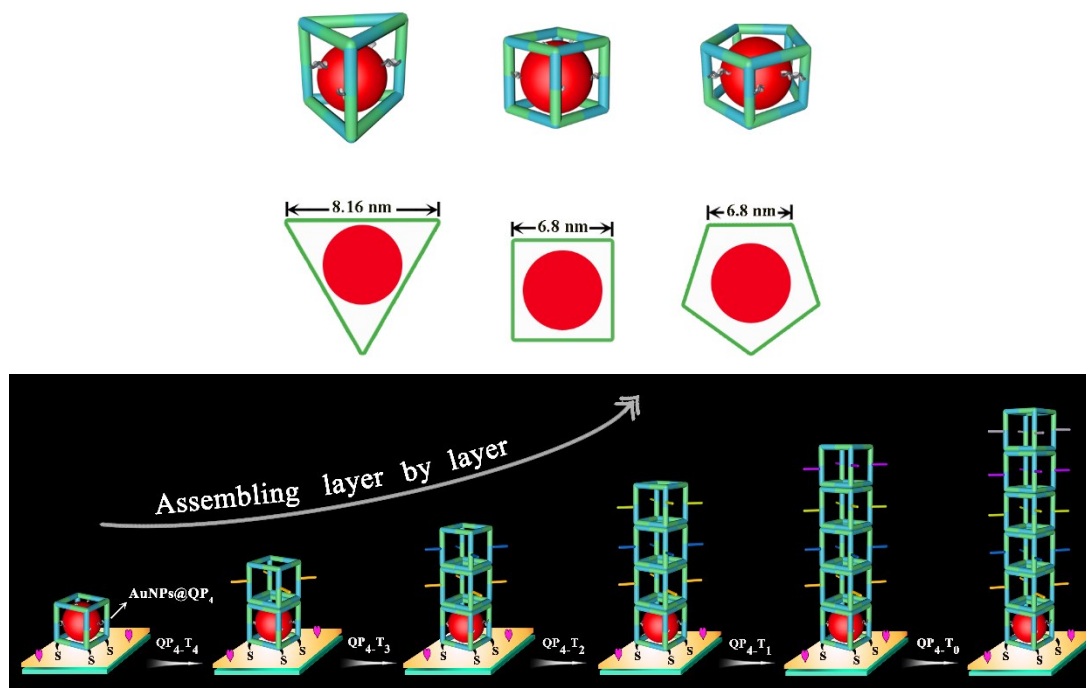
Scheme S2. Step-by-step assembly process of DNA nanopillars on electrodes.

Results and Discussion

Characterization of the Prepared Materials.

Transmission electron microscopy (TEM) was used to characterize the prepared AuNPs. Fig. S1A showed that the AuNPs displayed uniform spherical particles with an average diameter of 4 nm, implying the successful synthesis of AuNPs. In addition, the morphology of the DNA nanopillar was characterized by AFM. From Fig. S1B, we could see that AuNPs with height of ~5.1 nm was attached to the end of linear-shaped DNA nanostructure (~2.2 nm in height), which revealed the successful formation of the proposed nanopillar.
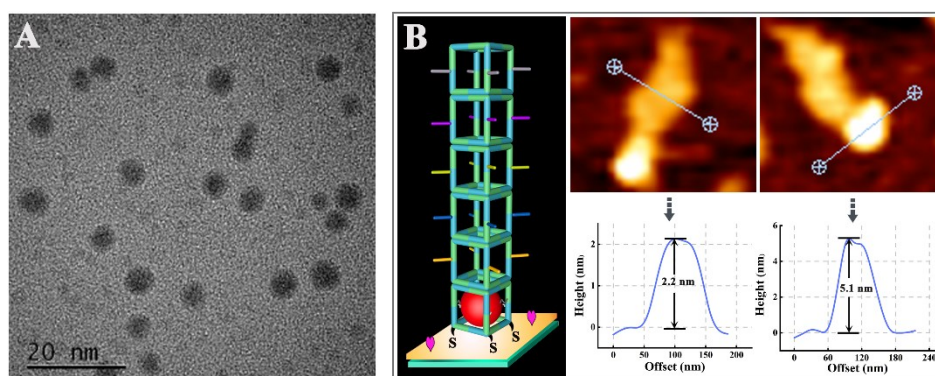

Fig. S1 (A) TEM images of the prepared AuNPs. (B) AFM images of DNA nanopillar.

Characterization of the Electrode Modification.

Cyclic voltammogram (CV) was utilized to characterize the stepwise fabrication processes of biosensor. As depicted in Fig. S2, the depAu modified electrode showed an obvious enhanced current (curve b) compared with that of the bare electrode (curve a), proving the superior conductivity of depAu. When AuNPs@quadrangular prism (AuNPs@QP$_4$) assembled on the GCE, the peak current decreased (curve c) due to the electron transfer obstruction of the complex. The current decreased significantly after incubating with blocking agent HT (curve d). Successive modification of QP$_4$

with different tracks resulted in a further reduced current (curve e), which can be attributed to the repulsion effect between the negatively charged phosphate backbone of the DNA and $[Fe(CN)_6]^{3-/4-}$. However, when bipedal DNA walker and corresponding fuels was introduced on the electrode, the current was increased (curve f) for the prominent electrochemical activity of hemin. These results confirmed that the superficial construction of proposed biosensor was successful.
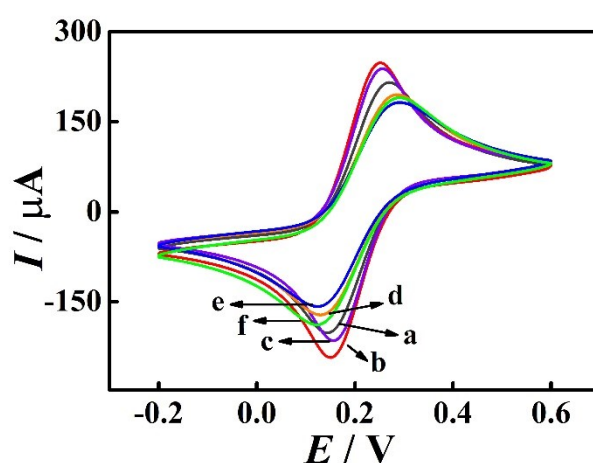

Fig. S2 Cyclic voltammograms of different interfacial processes in the 5 mM $[Fe(CN)_6]^{3-/4-}$ containing 0.1 M KCl. (a) bare GCE, (b) depAu/GCE, (c) QP$_4$@AuNPs/depAu/GCE, (d) HT/QP$_4$@AuNPs/depAu/GCE, (e) HT/QP$_4$@AuNPs/depAu/GCE after being treated with different DNA cages (f) step e incubated with bipedal DNA walker.

Enzyme Cascade Activity Based on Colorimetry.

We have further investigated the effect of interenzyme distance on the enzymatic cascade activity via colorimetric assay using glucose and TMB as the substrate. Specifically, AuNPs can catalyze glucose to produce gluconic acid and H_2O_2 in the presence of O_2. The in situ generated H_2O_2 can be used to oxidize TMB to produce the oxTMB with the help of hemin/G-quadruplex DNAzyme (Fig. S3A). The

absorbance values of oxTMB was recorded using an UV−vis spectrophotometer. As illustrated in Fig. S3B, negligible absorbance in the UV-vis absorption spectra was observed in the absence of cascade enzymes (curve a), suggesting that no oxidation reaction occurred in the mixture of glucose and TMB. After addition of AuNPs and hemin/G-quadruplex DNAzyme into the mixture of glucose and TMB for 30 min, the obtained solution showed a characteristic absorbance at 652 nm. Among them, 9.9 nm interenzyme distance (curve d) exhibited the strongest UV-vis absorption spectra compared with other interenzyme distance (curve b, c, and e), indicating superior cascade catalytic activity at an interenzyme distance of 9.9 nm. This result was consistent with Fig. 3B.
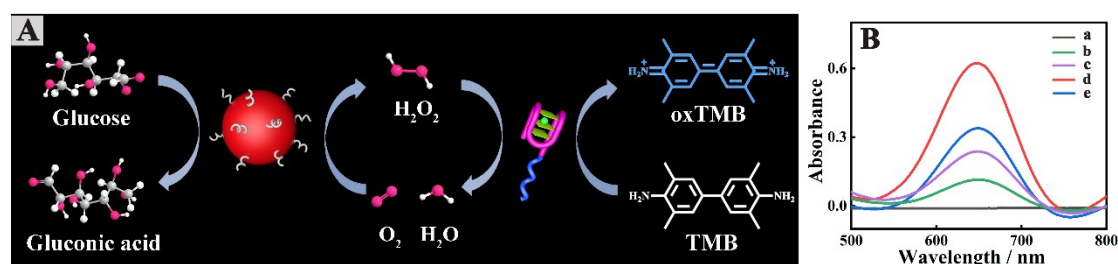

Fig. S3 (A) schematic illustration of the enzyme-mimetic cascade reaction. (B) UV-vis absorption spectra of various sample: (a) glucose + TMB, (b-e) glucose + TMB + cascaded enzymes (AuNPs and hemin/G-quadruplex DNAzyme) with different spacing, which were 3.3 nm, 6.6 nm, 9.9 nm, and 13.2 nm, respectively.

Construction of an Electrochemiluminescent 3D DNA Walking Nanomachine.

The mechanism of bipedal DNA walker was studied using electrochemiluminescence (ECL) analysis. As we all known, the distance between energy donor and acceptor is important for the efficiency of energy transfer. Herein, we designed a 3D DNA walking nanomachine, in which bipedal DNA walker was

labeled with the ECL emitter $Ru(bpy)_3^{2+}$, and AuNPs was labeled with the quencher AF. The separation distance between $Ru(bpy)_3^{2+}$ and AF can be systematically controlled though the top-down movement of bipedal DNA walker triggered by toehold mediated strand displacement reaction (Fig. S4A). As shown in Fig. S4B, the ECL gradually decreased along with the proximity between $Ru(bpy)_3^{2+}$ and AF. These results indicated the successful operation of the designed 3D DNA walking machine.
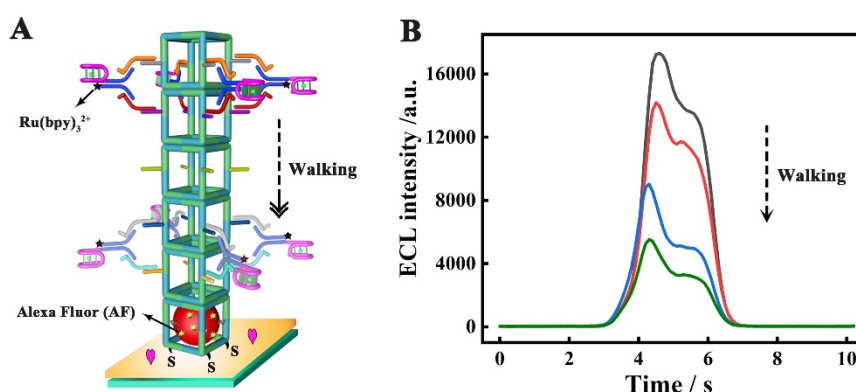

Fig. S4 (A) Schematic illustrating locomotion mechanism of the 3D DNA walking machine. (B) ECL responses of biosensor under various interenzyme distance induced by TSDR.

Table S2. Comparison of Some Reported Literatures for Pb^{2+} Detection.

Analytical method	Detection limit	Linear range	Ref.
Fluorescence	23.5 nM	100−600 nM	[1]
Fluorescence	2.89 nM	0−200 nM	[2]
Colorimetric	59.39 pM	0.1−15 nM	[3]
UV−vis	25.2 nM	0−14 μM	[4]
Electrochemical	0.019 ± 0.001 μM	0.5−2.2 μM	[5]
Electrochemical	0.03 nM	10 nM−10 μM	[6]
Electrochemical	21 nM	25 nM−10 μM	[7]
Electrochemical	2 pM	0.005−1000 nM	[8]
Electrochemical	0.03 nM	10 nM−10 μM	[9]
Electrochemical	5.5 nM	20 nM−10 mM	*This work*

Selectivity and Reproducibility of the Biosensor.

To determine the high specificity of proposed biosensor, 10-fold interference ions (200 μM) including Cr^{3+}, Cu^{2+}, Bi^{3+}, Ag^+ and Cd^{2+} were used to investigate. As shown in Fig. S5A, a negligible DPV response of interfering ions was observed compared with that of target Pb^{2+} (20 μM), which indicated that the sensing system had favorable specificity toward Pb^{2+}. Additionally, the inter-assays and intra-assays were performed to assess the reproducibility of biosensor and the results were displayed in Fig. S5B. The intra-assay precision was investigated by detecting 200 μM Pb^{2+} with three sensing electrode made in the same batch, and the relative standard deviation (RSD) was 3.9%. Moreover, the inter-assay precision was explored with the DPV responses of same sensing electrode incubated with 200 μM Pb^{2+} made in different batches, and the RSD value was 3.7%. The above results indicated that the proposed biosensor possessed an excellent reproducibility.
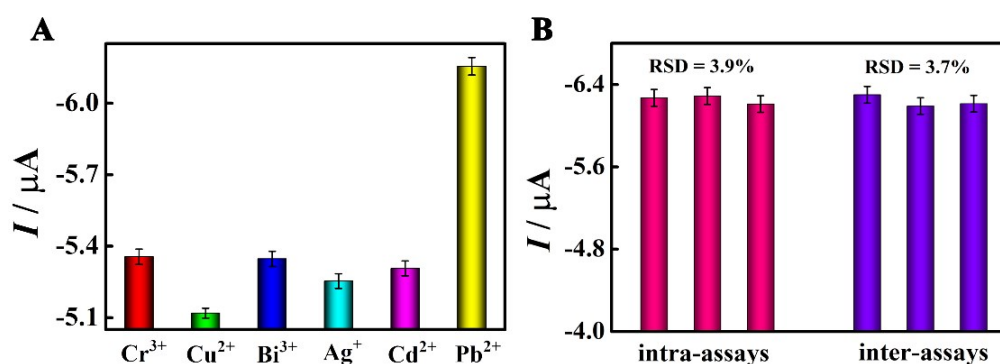

Fig. S5 (A) Selectivity of the proposed sensing system for Pb^{2+} assay. (B) Reproducibility of the proposed biosensors.

REFERENCES

(1) D. Peng, Y. Q. Li, Z. C. Huang, R. P. Liang, J. D. Qiu and J. W. Liu, *Anal. Chem.*, 2019, **91**, 11403-11408.

(2) H. Q. Wang, L. Yang, S. Y. Chu, B. H. Liu, Q. K. Zhang, L. M. Zou, S. M. Yu and C. L. Jiang, *Anal. Chem.*, 2019, **91**, 9292-9299.

(3) Z. J. Huang, J. M. Chen, Z. W. Luo, X. Q. Wang and Y. X. Duan, *Anal. Chem.*, 2019, **91**, 4806-4813.

(4) B. Wen, J. Q. Xue, X. J. Zhou, Q. W. Wu, J. J. Nie, J. T. Xu and B. Y. Du, *ACS Appl. Mater. Interfaces*, 2018, **10**, 25706-25716.

(5) M. B. Gumpu, U. M. Krishnan and J. B. B. Rayappan, *Anal Bioanal Chem.*, 2017, **409**, 4257-4266.

(6) R. j. Mo, L. He, C. X. Zhou, Z. J. Qian, P. Z. Hong, S. L. Sun, Z. Wang, Y. Wang and C. Y. Li, *Anal. Chem.*, 2019, **91**, 8184-8191.

(7) W. J. Kang, X. Pei, C. A. Rusinek, A. Bange, E. N. Haynes, W. R. Heineman and I. Papautsky, *Anal. Chem.*, 2017, **89**, 3345-3352.

(8) Y. J. Yu, C. Yu, Y. Z. Niu, J. Chen, Y. L. Zhao, Y. C. Zhang, R. F. Gao and J. L. He, Biosens. Bioelectron., 2018, **101**, 297-303.

(9) R. J. Mo, L. He, C. X. Zhou, Z. J. Qian, P. Z. Hong, S. L. Sun, Z. Wang, Y. Wang and C. Y. Li, *Anal. Chem.*, 2019, **91**, 8184-8191.